Toxicology Mechanisms and Methods

ISSN: (Print) (Online) Journal homepage: https://www.tandfonline.com/loi/itxm20

Aristolochic acid induces mitochondrial apoptosis through oxidative stress in rats, leading to liver damage

Yao Wang, Xianglin Ma, Chong Zhou, Yongzhen Jia, Si Liu, Zongliang Xiong, Xu Guo, Xue Fei, Xiaowen Jiang & Wenhui Yu

To cite this article: Yao Wang, Xianglin Ma, Chong Zhou, Yongzhen Jia, Si Liu, Zongliang Xiong, Xu Guo, Xue Fei, Xiaowen Jiang & Wenhui Yu (2021) Aristolochic acid induces mitochondrial apoptosis through oxidative stress in rats, leading to liver damage, Toxicology Mechanisms and Methods, 31:8, 609-618, DOI: 10.1080/15376516.2021.1946229

To link to this article: https://doi.org/10.1080/15376516.2021.1946229

Published online: 08 Aug 2021.

TOXICOLOGY MECHANISMS AND METHODS
2021, VOL. 31, NO. 8, 609–618
https://doi.org/10.1080/15376516.2021.1946229

Taylor & Francis
Taylor & Francis Group

RESEARCH ARTICLE

Aristolochic acid induces mitochondrial apoptosis through oxidative stress in rats, leading to liver damage

Yao Wang[a], Xianglin Ma[a], Chong Zhou[a], Yongzhen Jia[a], Si Liu[a], Zongliang Xiong[a], Xu Guo[a], Xue Fei[a], Xiaowen Jiang[a] and Wenhui Yu[a,b]

[a]Department of Veterinary Medicine, Northeast Agricultural University, Harbin, China; [b]Department of Veterinary Medicine and Key Laboratory of the Provincial Education Department of Heilongjiang for Common Animal Disease Prevention and Treatment, Northeast Agricultural University, Harbin, China

ABSTRACT

Aristolochic acid (AA) are persistent soil pollutants in the agricultural fields of the Balkan Peninsula. Preparations containing aristolochic acid are widely used for anti-inflammatory, diuretic, etc. To study the hepatotoxicity of aristolochic acid, 80 healthy SD rats were selected and divided into 20 mg/kg-AA group, 4 mg/kg-AA group, and 2 mg/kg-AA group and blank group, 20 rats per group. Mainly tested the body weight, liver function, liver tissue oxidative stress and pathological changes of liver tissue in rats. The ALT and AST activities in the serum of the rats in the administration groups were increased compared with the blank group. The activity of MDA in the administration groups was higher than that in the blank group; the activities of SOD, T-AOC and GSH-PX were significantly lower than those in the blank group. HE tissue sections also found that the administration groups showed varying degrees of hepatocyte boundary blur, nuclear fragmentation, and fibrosis tendency. Transmission electron microscopy showed that the mitochondria of the rat liver became more and more severely damaged with the increase of dose. Compared with the blank group, the mRNA expression of Bax, Caspase-9 and Caspase-3 in the administration groups were determined, while the mRNA expression of the Bcl-2 was increased. And compared with the blank control group, the expression levels of apoptotic proteins caspase-9 and caspase-3 increased significantly in the 20 mg/kg-AA group. Aristolochic acid can induce liver injury in rats through oxidative stress pathway and mitochondrial apoptosis pathway.

Abbreviation: AA: Aristolochic acid; SOD: Superoxide dismutase; MDA: Malondialdehyde; T-AOC: Total antioxidant capacity; GSH-PX: Glutathione Peroxidase; SD: Sprague Dawley; AST: aminotransferase Assay; ALT: Alanine aminotransferase Assay; HE: hematoxylin-eosin; MEK/ERK1/2: Mitogen-activated protein kinase/Extracellular regulated protein kinases 1/2

ARTICLE HISTORY
Received 21 April 2021
Revised 15 June 2021
Accepted 16 June 2021

KEYWORDS
Aristolochic acid; rat liver; toxicity; oxidative stress; mitochondrial apoptosis

1. Introduction

Aristolochic acid (AA) is a nitrophenanthrene organic acid compound, which is an effective ingredient in Chinese herbal medicines such as Aristolochia and Asarum. These herbs containing aristolochic acid are common in southern Brazil and India, and their leaf or stem-containing preparations are traditionally used as an anti-inflammatory, diuretic and anti-toxic antidote (Dey et al. 2020). Therefore, most Chinese medicines containing AA are mostly used to treat various diseases such as eczema, pneumonia, stroke, hepatitis, snake bites, arthritis, gout and coronary artery disease (Han et al. 2019). But in 1992, Belgians first discovered kidney disease in women who took aristolochic acid diet pills (Vanherweghem et al. 1993; Anandagoda and Lord 2015). In the following period, a large number of cases of kidney damage caused by aristolochic acid have been reported worldwide (Ding and Chen 2012). Therefore, AA causes kidney disease, and subsequent studies have also shown that aristolochic acid can cause kidney failure and upper urinary tract cancer. In 2013, in the US Science Translational Medicine report, aristolochic acid caused more mutations than tobacco, ultraviolet light and other carcinogens, and confirmed the correlation between aristolochic acid and liver cancer for the first time (Chwei-Shiun et al. 2000; Tanaka 2000; Schwabe and Luedde 2018).

Many studies have reported the carcinogenic effects of aristolochic acid on the kidneys, but few reported the toxic effects of aristolochic acid on the liver. Therefore, this experiment aims to study the toxic effect of aristolochic acid on rat liver. The extent of aristolochic acid liver injury was verified by tissue sectioning and electron microscopy, and liver damage was induced by oxidative stress and apoptosis. It

CONTACT Xiaowen Jiang jiangxiaowen@neau.edu.cn College of Veterinary Medicine, Northeast Agricultural University, Harbin 150030, China; Wen-hui Yu yuwenhui@neau.edu.cn Department of Veterinary Medicine and Key Laboratory of the Provincial Education Department of Heilongjiang for Common Animal Disease Prevention and Treatment, Northeast Agricultural University, Harbin 150030, China

provides a reference for the follow-up study on the treatment of poisoning caused by the AA.

2. Materials and methods

2.1. Materials

Sprague-Dawley rats(male) were purchased from Harbin Medical University, China. Aristolochic acid (≥95%) was purchased from Nanjing DASF Biotechnology Co. Ltd, China. Superoxide dismutase (SOD) assay kit (WST-1 method), Malondialdehyde (MDA) assay kit, Total antioxidant capacity(T-AOC) assay kit, Glutathione Peroxidase (GSH-PX) assay kit, and Aspartate aminotransferase Assay Kit and Alanine aminotransferase Assay Kit were purchased from Nanjing Jiancheng Bioengineering Institute, China. 2x SYBR Green qPCR Master Mix was purchased from Bimake, Houston, TX, USA. HiScript III RT SuperMix for qPCR was purchased from Vazyme Biotech Co.Ltd, China. TRIzol Reagent was purchased from Thermo Fisher Scientific, USA. LightCycler 480 Multiwell Plate 96 was purchased from Roche, German.

2.2. Methods

2.2.1. Drug intervention

Rats were maintained under SPF laboratory conditions on 12-hour light/dark cycles with free access to food and water. Eighty male SD rats weighing 180–220 g were randomly divided into four groups: blank group (Only DMSO), 20 mg/kg AA group, 4 mg/kg AA group, and 2 mg/kg AA group. Twenty rats in each group were randomly selected for the drug administration period test (intragastrical administration of AA for 28 days), and the remaining 10 were used as the drug withdrawal period test (After 28 days of intragastric administration, 2 weeks of withdrawal). All rats received intragastrical administration of AA dissolved in DMSO solution to the appropriate concentration for a duration. Rats in the Blank group were given an equivalent volume of DMSO (2 mL/kg).

2.2.2. Effect of aristolochic acid on body weight and organ coefficient in rats

The body weight of each rat was weighed on the 1d, 7d, 14d, 21d, 28d, 35d, and 42d of the test. On the 28th day of the experiment, 10 rats in each group were randomly selected and sacrificed after blood collection, and the liver coefficient was measured. On the 42nd day, the remaining 10 rats were sacrificed after blood collection, and the liver coefficient was also measured.

2.2.3. Determination of liver injury index

Accurately weighed 0.1000 g of liver tissue, added 0.9 mL of physiological saline, homogenized with a homogenizer under ice water bath conditions, made 10% tissue homogenate, centrifuged at 2500 r/min for 10 minutes, and removed the supernatant. A portion of the tissue homogenate was taken and the protein concentration was determined. The rest were measured strictly according to the Aspartate aminotransferase Assay (AST) Kit and Alanine aminotransferase Assay (ALT) kits.

2.2.4. Determination of liver oxidative stress index

Accurately weighed 1.0000 g of tissue, added 0.9 mL of normal saline, and made 10% tissue homogenate under ice water bath condition. Took a part and measured it strictly according to the instructions of the malondialdehyde (MDA) kit. The assay is performed in strict accordance with the requirements of superoxide dismutase (SOD), glutathione peroxidase (GSH-PX), and total antioxidant capacity (T-AOC) kits.

2.2.5. HE staining

The liver tissue was fixed in 4% paraformaldehyde and cut into coin-sized tissue slices. After the tissue gradient ethanol dehydration and xylene transparency were performed for 20 minutes, they were immersed in wax at 58 °C for 1.5 hours. Then embed it with melted paraffin, and after the wax liquid has solidified, it is fixed on the holder to trim the wax block. Slicing with a slicing machine, showing the slices, removing the slices, and drying in the oven overnight. Then use xylene, gradient ethanol, and water for dewaxing. After staining with hematoxylin for 15 minutes, wash with distilled water for a few seconds, differentiate with 1% alcohol and hydrochloric acid for 2–3 seconds, rinse with running water for 2 hours, stained with 5% eosin for 10 minutes, and rinse with water for 30 seconds. Finally, perform ethanol gradient dehydration, transparent xylene, resin sealing, and oven drying. The stained sections were analyzed under a light microscope at 400 magnification (Jiang et al. 2017; Chi et al. 2021).

2.2.6. Ultrastructural observations

The liver was cut into 1 cm cubes, placed in 2.5% glutaraldehyde, and placed in the refrigerator (4 °C) for 7 days. The fixed sample was rinsed with 0.1 mol/L phosphate buffer, post-fixed in 1% osmium tetroxide, and rinsed again. The next step was dehydration (50% ethanol, 70% ethanol, 90% ethanol for 10 minutes, 100% ethanol for 10 minutes, twice, then 100% ethanol and 100% acetone 1:1, 10 minutes, 100% acetone, room temperature for 5 minutes, immersion through the night), embedding (pure acetone and embedding solution 1:1 at room temperature for 40 minutes, in pure acetone and embedding solution 1:2, 2 h, then pure acetone and embedding solution 1:3, overnight), followed by polymerization, trimming, sectioning (50–60 nm) (Cui et al. 2019). Liver ultrathin sections were then stained with uranyl acetate and examined under a transmission electron microscope (Hitachi 7650, Tokyo, Japan).

Table 1. Primer sequence.

Gene	Accession numbers	Primer (5′-3′)	Amplicon sizes
Bax	NM_017059.2	5′-CACGTCTGCGGGGAGTCAC-3′ 3′-TAGAAAAGGGCAACCACCCG-5′	419
Bcl-2	NM_016993.2	5′-TCGCGACTTTGCAGAGATGT-3′ 3′-CAATCCTCCCCCAGTTCACC-5′	116
Caspase-9	NM_001277932.1	5′-ACCTTCCCAGGTTGCCAATG-3′ 3′-GCTGCTAGGAGCATGTTTGC-5′	251
Caspase-3	NM_001284409.1	5′-GAGCTTGGAACGGTACGCTAA-3′ 3′-GAGTCCACTGACTTGCTCCC-5′	118
GAPDH	NM_017008.4	5′ -GGCGGTACAACTCAGGTTCC-3′ 3′-ATCCGTTCACACCGACCTTC-5′	145

Table 2. Dilutions of antibodies.

Antibodies	Source	Dilution factor
caspase-9	Wanleibio (Shen Yang, China)	1:500
caspase-3	Wanleibio (Shen Yang, China)	1:500
GAPDH	Biosynthesis Biotechnology (Bei Jing, China)	1:1000

2.2.7. Bax, bcl-2, caspase-9, caspase-3 mRNA expression detection using qRT-PCR

Fifty milligram of liver tissue was weighed and ground in a homogenizer with 1 mL Trizol. The total RNA was extracted and the cDNA was synthesized. The RT-PCR primers were designed based upon the NCBI rat mRNA sequence database (Table 1). After the primers were synthesized (by Shanghai Shenggong Biological Co., Ltd), the RT-PCR reaction system was prepared according to the requirements of the 2x SYBR Green qPCR Master Mix kit. The relative level of mRNA was calculated according to the $2^{-\Delta\Delta Ct}$ method (Hu et al. 2019). GAPDH could be used as an endogenous control for standardization.

2.2.8. Western blotting to detect the expression of caspase3 and caspase9 in liver tissue

The total protein of liver tissue was extracted and subjected to 10% SDS-PAGE electrophoresis, and then the sample was transferred to the PVDF membrane. The PVDF membrane was sealed with 5% skimmed milk at room temperature for 2 hours and then placed in a proportionally diluted primary antibody (the antibody name, manufacturer and dilution factor are shown in Table 2). The samples were incubated overnight in a refrigerator at 4 °C. Then, the membrane was placed in goat anti-rabbit HRP at a dilution ratio of 1/5000, incubated at 37 °C for 2 hours, rinsed, and then exposed to light. The Tianneng gel imaging system is used for image acquisition. Image analysis uses Image J software for optical density (OD) analysis, relative protein expression = target protein OD value/GAPDH OD value (Chi et al. 2021).

2.3. Statistical analysis

Data were expressed as means ± SEM and analyzed with SPSS 22.0 (SPSS, Chicago, IL, USA). Oneway ANOVA with LSD or Dunnet'T3 tests were applied to evaluate the statistical significance of differences between the experimental groups and controls. $P < 0.05$ was considered statistically significant.

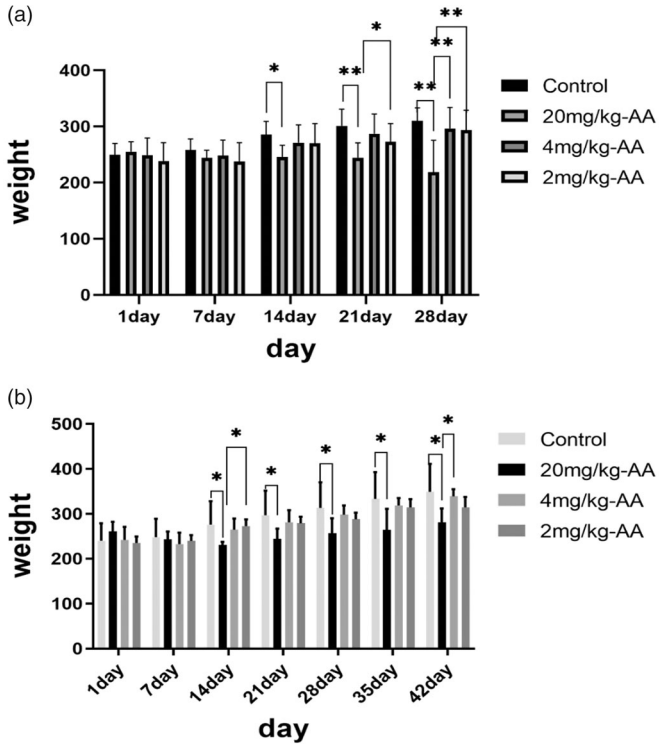

Figure 1. Effect of aristolochic acid on body weight of experimental group(a) and recovery group(b). (N = 10) "*" Significant compared with respective control; $P < 0.05$. "**" Significant compared with respective control; $P < 0.01$.

3. Results

3.1. Effect of aristolochic acid on body weight of rats

On the 14th day, the 20 mg/kg-AA dose group has a significant difference in the weight of rats compared with the blank group. With the prolonged administration time, the difference is extremely significant. However, the doses of 4 mg/kg-AA dose group and 2 mg/kg-AA dose group were not significantly different from the blank group (Figure 1a). After 28 days of the administration, the bodyweight of the 20 mg/kg-AA group rats recovered during 2 weeks of drug withdrawal, and the difference was significant compared with the blank group; the difference between the 4 mg/kg-AA and 2 mg/kg-AA groups was not significant (Figure 1b).

3.2. The result of liver function test

Compared with the blank group, the ALT activity of the 20 mg/kg-AA group of aristolochic acid was significantly higher than that of the blank group ($P < 0.05$). The 4 mg/kg-AA group was also significantly higher than the blank group ($P < 0.05$). The 2 mg/kg-AA group had higher ALT activity than the blank group ($P < 0.05$) (Figure 2a).

After 14 days of recovery test, the recovery group and the experimental group have the same trend, Therefore, liver damage caused by aristolochic acid cannot be recovered within a short time (Figure 2b). The AST activity of the 20 mg/kg-AA group of aristolochic acid was significantly higher than the blank group ($P < 0.01$), and the 4 mg/kg-AA group was also significantly increased ($P < 0.05$). The 2 mg/

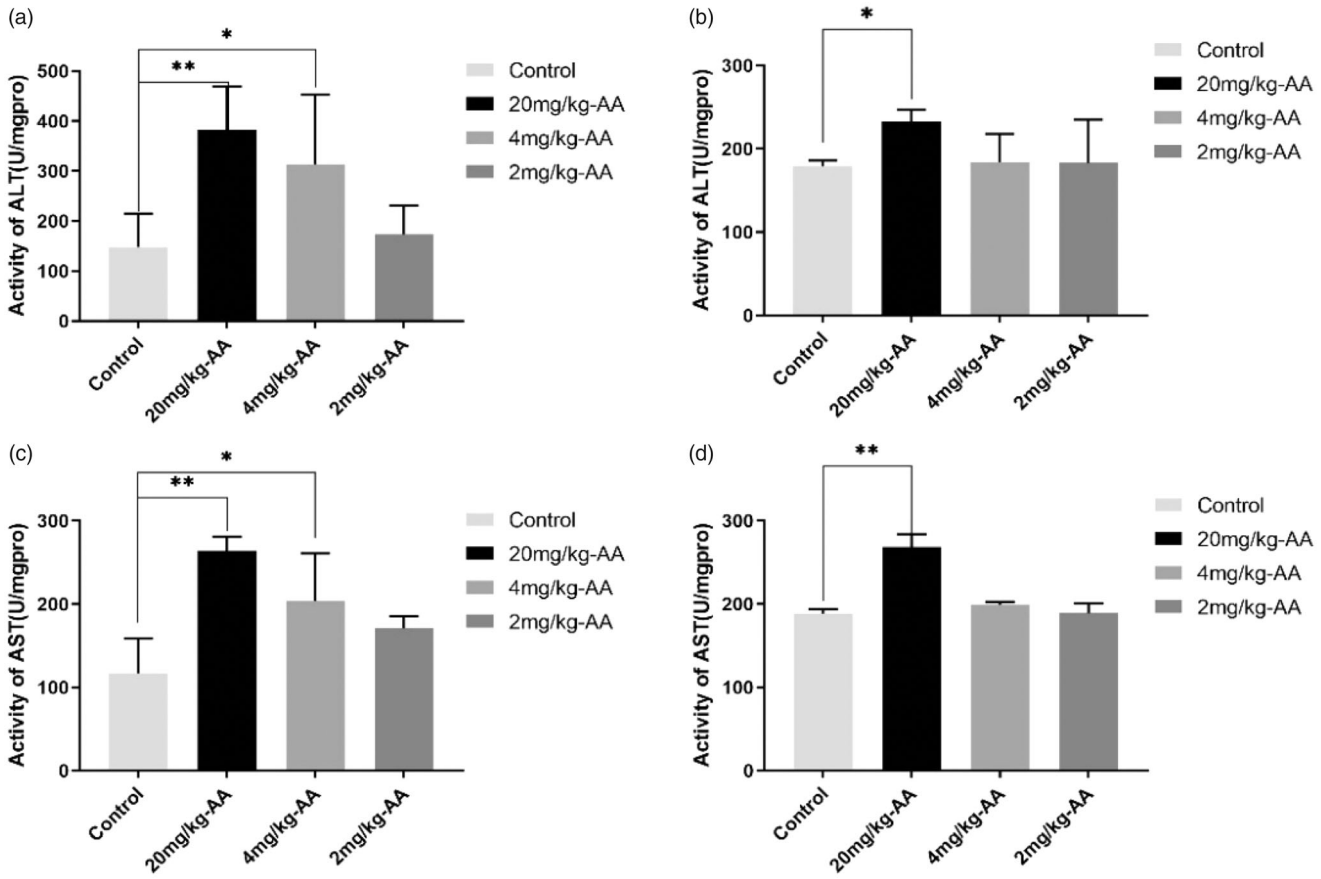

Figure 2. Effect of aristolochic acid on ALT activity in rats of the experimental group (a) and recovery group (b) were measured using ELISA. And the effect of aristolochic acid on AST activity in rats of experimental group (c) and recovery group (d) were measured using ELISA. Data are expressed as mean ± SEM of three separate experiments. '*' Significant compared with respective control; $P < 0.05$. '**' Significant compared with respective control; $P < 0.01$.

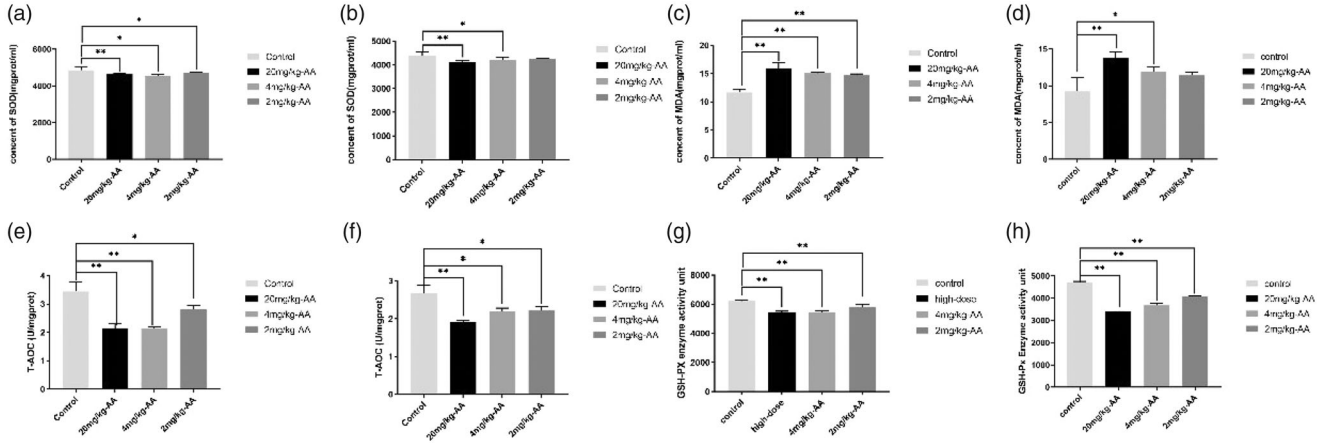

Figure 3. (a) SOD activity in rats liver during drug delivery; (b) SOD activity in rats liver during withdrawal period; (c) MAD activity in rats liver during drug delivery; (d) MAD activity in rats liver during withdrawal period; (e) T-AOC activity in rats liver during drug delivery; (f) T-AOC activity in rats liver during withdrawal period; (g) GSH-Px activity in rats liver during drug delivery; (h) GSH-Px activity in rats liver during the withdrawal period. Data are expressed as mean ± SEM of three separate experiments. *Significant compared with respective control; $P < 0.05$. '*' Significant compared with respective control; $P < 0.05$. '**' Significant compared with respective control; $P < 0.01$.

kg-AA group had higher AST activity than the blank group but no significant differences (Figure 2c). After 14 days of recovery test, the recovery group and the experimental group trend were similar, but the 2 mg/kg-AA group had a reduction in the content (Figure 2d). Therefore, after the aristolochic acid damage the liver, the 2 mg/kg-AA group recovered.

3.3. The result of oxidative stress level detection

Detection of oxidative stress-related indicators have shown that compared with the blank group, the 20 mg/kg-AA group, the 4 mg/kg-AA group, and the 2 mg/kg-AA group had decreased SOD activity, increased MDA activity, decreased T-AOC activity, and decreased GSH-Px activity. Therefore, aristolochic acid caused damage to the liver of

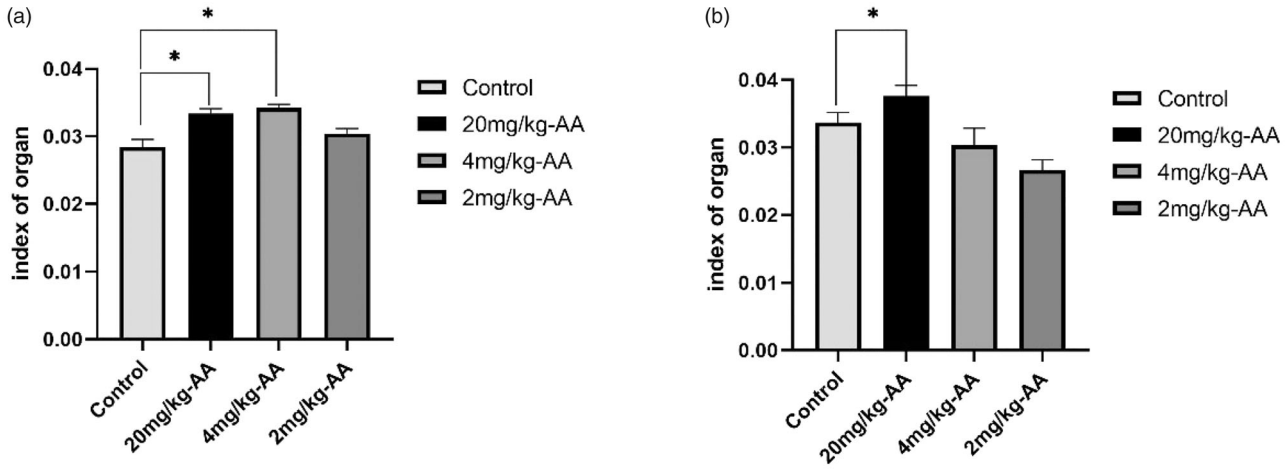

Figure 4. Effect of aristolochic acid on the liver coefficient of the experimental group(a) and recovery group(b). ($N = 10$) '*' Significant compared with blank group; $P < 0.05$.

rats and showed a dose-dependent effect. After 14 days of recovery trials, the recovery group had the same trend as the experimental group (Figure 3).

3.4. Effect of aristolochic acid on liver coefficient

In the 20 mg/kg-AA and 4 mg/kg-AA groups, the liver coefficient was significantly different from that in the blank group (Figure 4a). After 2 weeks of withdrawal, only the 20 mg/kg-AA group was significantly different from the blank group, while the 4 mg/kg-AA and 2 mg/kg-AA groups were not significantly different from the blank group (Figure 4b).

3.5. HE staining observation

The liver tissue of the blank group was slightly hyperemia, and the liver cell nucleus was dissolved (Figure 5a). In the 20 mg/kg-AA group, the hepatic cord structure was unclear, with mild fibrosis around the blood vessels, blurred hepatocyte boundaries, nuclear fragmentation, (Figure 5b). In the 4 mg/kg-AA group, the hepatocyte boundary was blurred, the nucleus was fragmented, there was a tendency to fibrosis (Figure 5c). In the 2 mg/kg-AA group, the hepatocyte boundary was unclear, hyperemia, mild fibrosis (Figure 5d).

After 2 weeks of withdrawal, the borders of the hepatocytes in the blank group were unclear, the nucleus was dissolved, and the tissue was slightly congested (Figure 5e). Moderate fibrosis around the central vein in the 20 mg/kg-AA group, vascular congestion, bile duct hyperplasia, loss of hepatic cord structure; fibrosis around the vein, thickening of the vessel wall, and intravascular congestion (Figure 5f). In the 4 mg/kg-AA group, hepatocyte interstitial enlargement and congestion, hepatocyte necrosis, and tissue congestion (Figure 5g). Hepatocyte necrosis in the 2 mg/kg-AA group, perivascular fibrosis, unclear cell boundaries; tissue congestion, nuclear fragmentation (Figure 5h).

3.6. Electron microscopic observation

Apoptosis has its unique morphological characteristics, including chromatin condensation and nuclear division, cell contraction, plasma membrane blistering, and the formation of apoptotic bodies. In the blank group, the mitochondria, endoplasmic reticulum, ribosomes and other organelles around the nucleus of rat liver cells were clearly visible, the nucleus and cytoplasm were separated, the cell membrane was intact, and there was no blistering (Figure 6a). However, the 20 mg/kg-AA dose group, the 4 mg/kg-AA dose group, and the 2 mg/kg-AA dose group showed different degrees of chromatin condensation and nuclear division, cell contraction, and plasma membrane blistering in hepatocytes (Figure 6). It can be seen that aristolochic acid has a damaging effect on rat liver cell in a dose-dependent manner.

3.7. Detection results of Bax, bcl-2, caspase-9 and caspase-3 mRNA expression levels in the liver

The detection of apoptotic genes showed that compared with the blank group, the mRNA expressions of Bax, Caspase-9 and Caspase-3 in the 20 mg/kg-AA group, the 4 mg/kg-AA group and the 2 mg/kg-AA group increased, and the mRNA expression of Bcl-2 decreased ($P < 0.05$ or $P < 0.01$) (Figure 7).

3.8. Detection results of caspase-9 and caspase-3 protein expression levels in the liver

Detection of apoptosis marker protein showed that compared with the blank group, the Caspase-9 and Caspase-3 protein expressions in the 20 mg/kg-AA dose group were significantly increased. ($P < 0.05$ or $P < 0.01$) (Figure 8).

4. Discussion

From the analysis of the chronic toxicity of aristolochic acid in rats, the weight of rats in the 20 mg/kg AA group of aristolochic acid has decreased. After 14 days of the

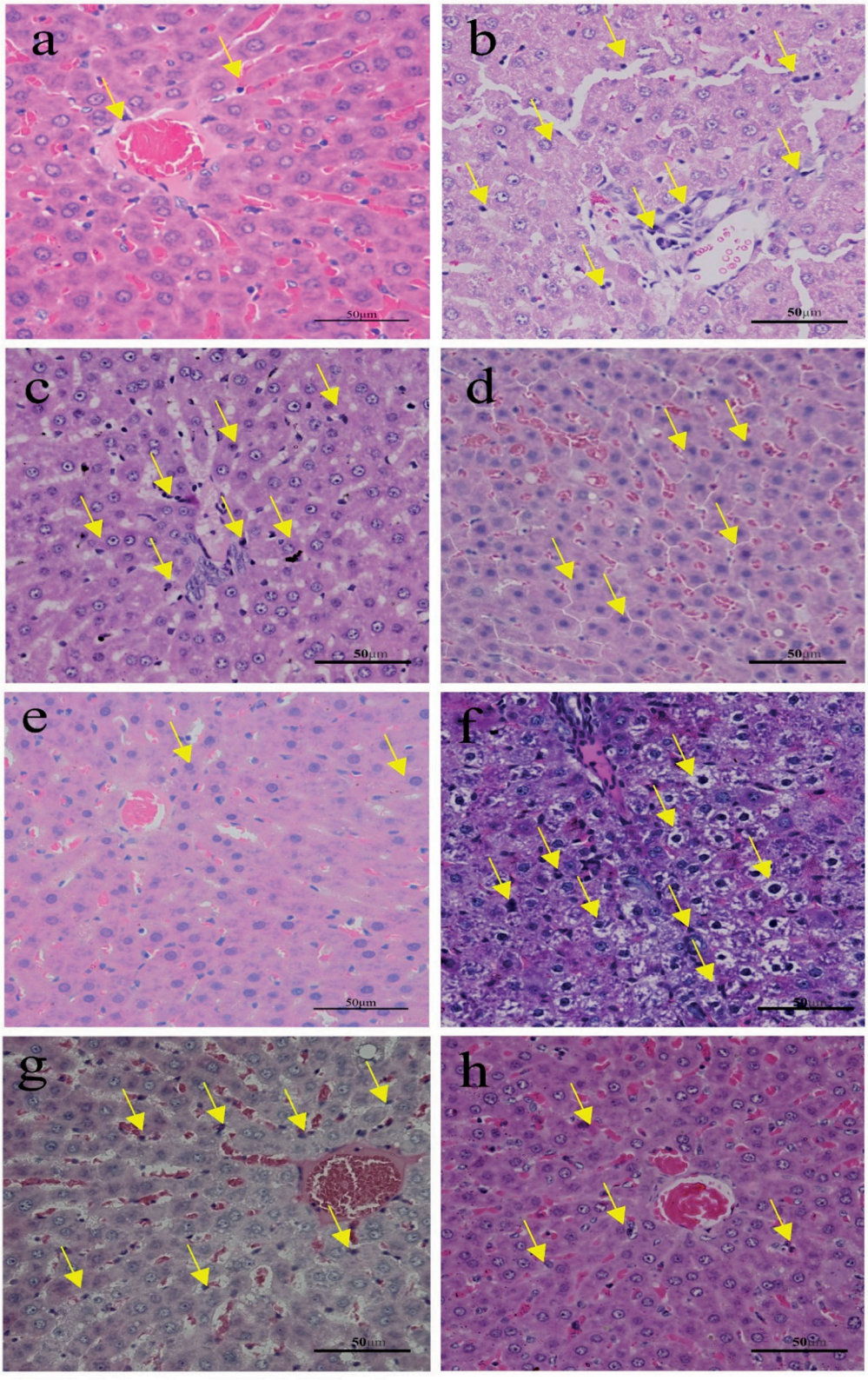

Figure 5. HE staining of rat liver injury by aristolochic acid. (x400) (a)control group: Liver tissue has a slight congestion. (b) 20 mg/kg-AA group: Hepatic cord structure is unclear, mild fibrosis around the blood vessels; hepatocyte boundary is blurred, nuclear fragmentation, fibrosis tendency. (c) 4 mg/kg-AA group: Hepatocyte borders are blurred, the nuclear nucleus is fragmented, and there is a tendency to fibrosis. (d) 2 mg/kg-AA group: Hepatocyte borders are unclear, congested, and mildly fibrotic. (e) blank group of recovery group: the nucleus was dissolved, and the tissue was slightly congested. (f) 20 mg/kg-AA group of recovery group: Moderate fibrosis around the central vein. (g) 4 mg/kg-AA group of recovery group: hepatocyte interstitial enlargement and congestion. (h) 2 mg/kg-AA group of recovery group: hepatocyte necrosis, perivascular fibrosis, unclear cell boundaries. Yellow arrow: inflammatory cells.

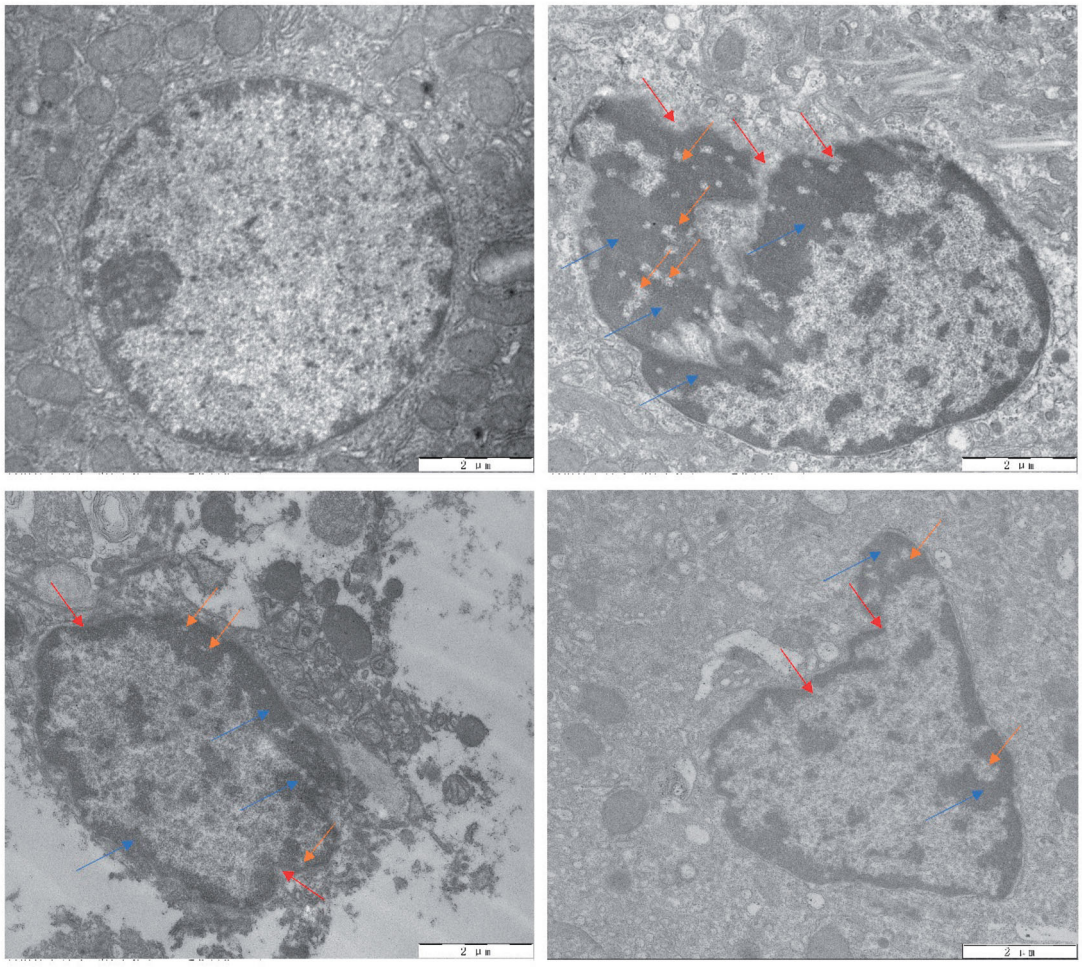

Figure 6. Transmission electron microscopic analysis of aristolochic acid on liver injury in rats. (x15000) Scale bars 2 μm. (a) control group: The chromatin is not concentrated, the cells are not contracted, and the plasma membrane does not bubble. (b) 20 mg/kg-AA group: There is a large area of chromatin condensation, cell shrinkage, and plasma membrane blistering. (c) 4 mg/kg-AA group: The emergence of chromatin condensation, cell shrinkage, membrane blistering. (d) 2 mg/kg-AA group: The cells shrink obviously, with slight chromatin condensation and plasma membrane blistering. The cells shrink obviously, with slight chromatin condensation and plasma membrane blistering. Red arrows indicate cell shrinkage, orange arrows indicate: cytoplasmic membrane blistering, blue arrows indicate: chromatin concentration.

administration, the body weight was significantly different from that of the blank group. Aristolochic acid is toxic to rats, affecting the metabolism and causing weight loss. Combined with the liver organ coefficient, the rats in the 20 mg/kg-AA group and the middle-dose group were significantly different from the blank group, indicating that aristolochic acid caused liver damage in rats, which affected liver metabolism.

Electron microscopic observation of the liver tissue of rats in each group of the experimental group showed that the mitochondrial structure around the hepatocytes was broken, and the organelles such as endoplasmic reticulum and ribosome were reduced. Studies have shown that the herbs containing aristolochic acid and AA can cause similar damage to the mitochondria in the kidneys of mice (Quan et al. 2020). This result is consistent with the result of hepatocyte nuclear division in the 20 mg/kg AA dose group in HE staining. In the 2 mg/kg-AA HE staining group, a small amount of fibrosis tendency, tissue congestion, and inflammatory cell infiltration was observed. In the 4 mg/kg-AA group, fibrosis tendency, some inflammatory cell infiltration, and a small amount of congestion in the venous sinus were also observed. In the 20 mg/kg-AA group, there was obvious inflammatory cell infiltration, nuclear fragmentation, and fibrosis tendency. It indicates that aristolochic acid can cause hepatocyte necrosis, which in turn affects the metabolism function of hepatocytes. Long-term use of aristolochic acid in a large amount of liver damage is more serious and will be dose-dependent. This result proves that indeed 20 mg/kg AAs of aristolochic acid can cause liver damage, and on October 18, 2017, researchers from Singapore and Taiwan published a paper claiming that aristolochic acid and its derivatives are widely involved in liver cancer in Taiwan and throughout Asia (Ng et al. 2017). And the literature proves that aristolochic acid metabolism can be left in the liver of rats (Ouyang et al. 2019). The results of liver damage indexes AST and ALT (Elangovan et al. 2019; Gao et al. 2019; Mohamed et al. 2019) showed that the concentrations of AST and ALT in the serum of rats in different dose groups were significantly higher than those in the blank group, and a dose-dependent aristolochic acid was observed. The 20 mg/kg-AA dose group had the highest serum AST and ALT, so the 20 mg/kg-AA AA was the most serious for the damage of rat liver.

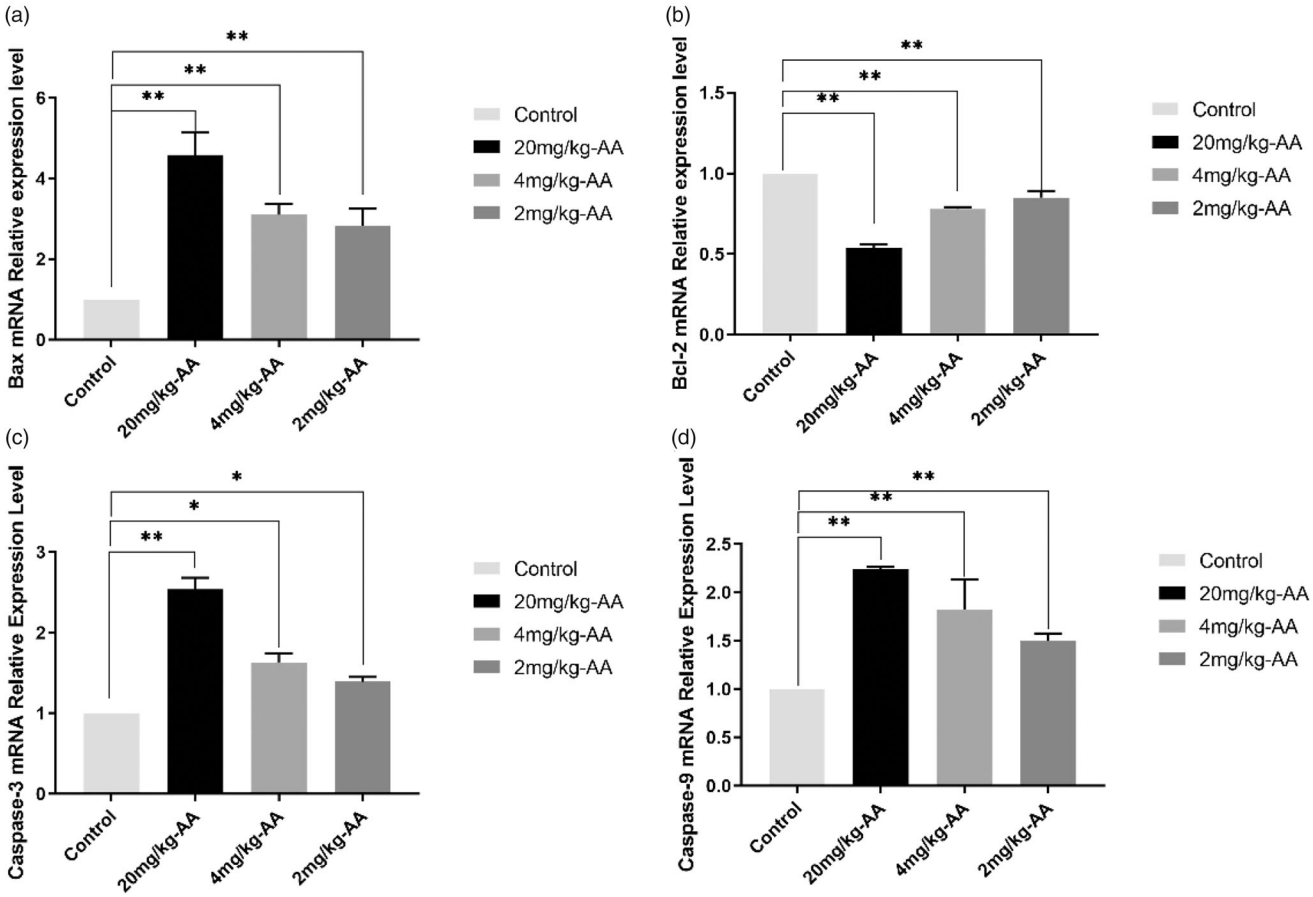

Figure 7. The mRNA expression of (a) Bax, (b) Bcl-2, (c) Caspase-3, (d) Caspase-9 in the rats liver. Data are expressed as mean ± SEM of three separate experiments. '*' Significant compared with respective control; $P < 0.05$. '**' Significant compared with respective control; $P < 0.01$.

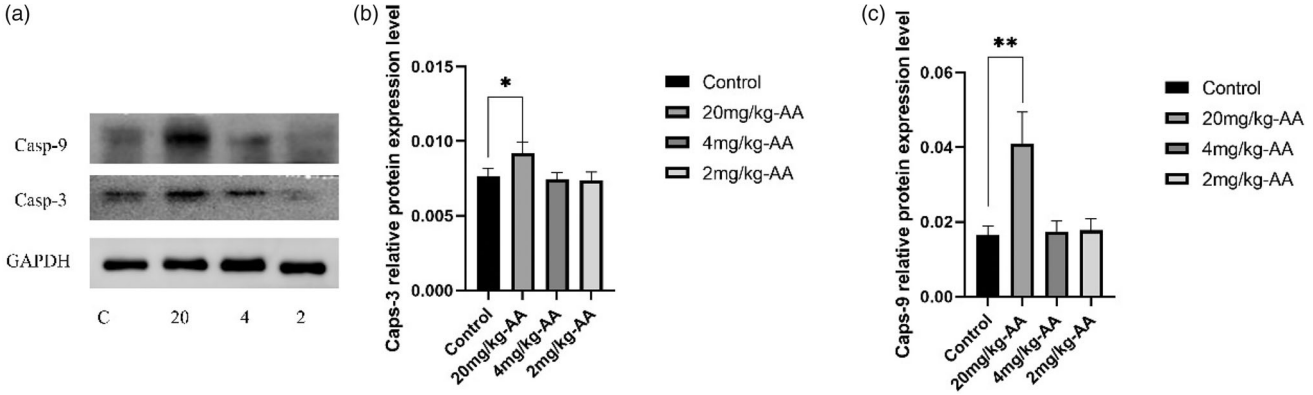

Figure 8. (a) Relative protein content (b) Caspase-3 Relative protein level (c) Caspase-9 Relative protein level. In Figure (a), c represents control group, 20 represents 20 mg/kg-AA, 4 represents 4 mg/kg-AA, 2 represents 2 mg/kg-AA. Data are expressed as mean ± SEM of three separate experiments. '*': ($P < 0.05$), '**': ($P < 0.01$).

Oxidative stress damage is one of the main factors that cause pathological changes in many organisms, and the location is mainly mitochondria (Hyung and Kim 2018; Khalaf et al. 2020), and many studies on the mechanism of aristolochic acid-induced nephropathy have shown that AA activates mitogen-activated protein kinase/extracellular regulated protein kinases 1/2 (MEK/ERK1/2) signaling pathway induces oxidative stress to cause DNA damage and consumes intracellular glutathione (GSH), leading to cytotoxicity and oxidative damage (Li et al. 2012; Anger et al. 2020). Studies have shown that AA exposure can increase the production of ROS (Romanov et al. 2015), cause oxidative damage and cause kidney disease, and studies have shown that aristolochic acid can cause kidney damage in mice through oxidative stress (Fan et al. 2021; Wang et al. 2021). At present, there is no research on the oxidative stress caused by AA in the liver. Therefore, the results of this experiment show that AA induced an increase in malondialdehyde (MDA) levels and a decrease in total antioxidant capacity (T-AOC) levels as well as superoxide dismutase (SOD) levels and antioxidant

enzymes glutathione peroxidase (GSH-Px), indicating that the rat liver had oxidative damage.

Oxidative stress can cause cell apoptosis, and the mitochondrial-mediated apoptosis pathway is one of the most classic apoptosis pathways (Green and Kroemer 2004; Sinha et al. 2013). Many environmental or chemical factors can activate the 'endogenous apoptotic pathway'/the mitochondrial pathway, such as ionizing radiation, Ultraviolet radiation, H_2O_2 el.at (Hu et al. 2019). These factors can cause cellular oxidative stress and activate the mitochondrial apoptotic pathway (Oakes 2020). Electron microscopy showed that aristolochic acid can cause decreased mitochondria and apoptotic cells, and the process of apoptosis is strictly controlled, such as the Bcl-2 family and Caspase family (Ku et al. 2011). The Bax protein is a member of the Bcl-2 family and normally forms a homologous or heterodimeric with Bcl-2, regulating apoptosis (Chipuk et al. 2010; Martinou and Youle 2011). The expression of Bax in the process of apoptosis is opposite to the expression of Bcl-2 (Singh et al. 2019). Bax promotes cell apoptosis, while Bcl-2 inhibits cell apoptosis. The experimental results showed that the Bax mRNA transcription level of the aristolochic acid group was higher than that of the blank group, while the transcription level of Bcl-2 mRNA was lower than that of the blank group. It shows that aristolochic acid increases the mRNA transcription level of Bax and reduces the mRNA transcription level of Bcl-2 to induce cell apoptosis. The activation of the anti-apoptotic gene Bcl-2 can prevent Bax from destroying the inner mitochondrial membrane and prevent the activation of Caspase precursors (Lakhani et al. 2006; Huang et al. 2011; Li et al. 2021). As an important member of the Caspase family, Caspase-3 is a terminal cleavage enzyme that plays an extremely important role in mediating apoptosis and is a marker of apoptosis (Lauber et al. 2003; Wu and Bratton 2013; Hassanen et al. 2021). The experimental results showed that the mRNA transcription levels of Caspase-9 and Caspase-3 mRNA in the aristolochic acid group were significantly higher than those in the blank group, and there were significant differences. In the protein expression level, only the 20 mg/kg AA group and the blank control group have significant differences. Therefore, aristolochic acid induces mitochondrial apoptosis by reducing Bax and increasing the transcription level of Bcl-2, thereby causing the increase of the protein levels of Caspase-9 and Caspase-3, leading to liver damage.

5. Conclusion

In this experiment, rats were subjected to a toxicity test with different doses of aristolochic acid. The results showed that aristolochic acid caused mitochondrial disruption in the rat liver, decreased organelles such as endoplasmic reticulum and ribosome and caused inflammatory cell infiltration and fibrosis tendency in the liver. The damage caused to the rat liver is produced by the mitochondrial pathway of apoptosis and oxidative stress.

Ethical approval

All of the procedures used in this study were approved by the Institutional Animal Care and Use Committee of Northeast Agricultural University.

Disclosure statement

The authors declare that they have no known competing financial interests or personal relationships that could have appeared to influence the work reported in this paper.

Funding

This work was supported by National Natural Science Foundation of China [NSFC-32072909].

Data availability statement

Datasets analyzed during the current study are available from the corresponding author on reasonable request.

References

Anandagoda N, Lord GM. 2015. Preventing aristolochic acid nephropathy. Clin J Am Soc Nephrol. 10(2):167–168.

Anger EE, Yu F, Li J. 2020. Aristolochic acid-induced nephrotoxicity: molecular mechanisms and potential protective approaches. IJMS. 21(3):1157.

Chi Q, Hu X, Zhao B, Zhang Q, Zhang K, Li S. 2021. Regulation of H2S-induced necroptosis and inflammation in broiler bursa of Fabricius by the miR-15b-5p/TGFBR3 axis and the involvement of oxidative stress in this process. J Hazard Mater. 406:124682.

Chi Q, Zhang Q, Lu Y, Zhang Y, Xu S, Li S. 2021. Roles of selenoprotein S in reactive oxygen species-dependent neutrophil extracellular trap formation induced by selenium-deficient arteritis. Redox Biol. 44: 102003–102003.

Chipuk JE, Moldoveanu T, Llambi F, Parsons MJ, Green DR. 2010. The BCL-2 family reunion. Mol Cell. 37(3):299–310.

Chwei-Shiun Y, and, Ching-Hao L, and, Shu-Horng C, and, 2000. Rapidly progressive fibrosing interstitial nephritis associated with Chinese herbal drugs - ScienceDirect. Am J Kidney Dis. 35:313–318.

Cui Y, Chang R, Zhang T, Zhou X, Wang Q, Gao H, Hou L, Loor JJ, Xu C. 2019. Chinese herbal formula (CHF03) attenuates non-alcoholic fatty liver disease (NAFLD) through inhibiting lipogenesis and anti-oxidation mechanisms. Front Pharmacol. 10:1190.

Dey A, Hazra AK, Mukherjee A, Nandy S, Pandey DK. 2020. Chemotaxonomy of the ethnic antidote Aristolochia indica for aristolochic acid content: Implications of anti-phospholipase activity and genotoxicity study. J Ethnopharmacol. 266:113416.

Ding YJ, Chen YH. 2012. Developmental nephrotoxicity of aristolochic acid in a zebrafish model. Toxicol Appl Pharmacol. 261(1):59–65.

Elangovan A, Subramanian A, Durairaj S, Ramachandran J, Lakshmanan DK, Ravichandran G, Nambirajan G, Thilagar S. 2019. Antidiabetic and hypolipidemic efficacy of skin and seed extracts of Momordica cymbalaria on alloxan induced diabetic model in rats. J Ethnopharmacol. 241:111989.

Fan Y, Elyce O, Frank YM, Khai GL, Greg HT, Xiaoyun J, and David JN-P. 2021. 'c-Jun amino terminal kinase signaling promotes aristolochic acid-induced acute kidney injury'. Front Physiol. 12:599114.

Gao Z, Yuan FF, Li HP, Feng YB, Zhang YW, Zhang C, Zhang JJ, Song Z, Jia L. 2019. The ameliorations of Ganoderma applanatum residue polysaccharides against CCl4 induced liver injury. Int J Biol Macromol. 137:1130–1140.

Green DR, Kroemer G. 2004. The pathophysiology of mitochondrial cell death. Science. 305(5684):626–629.

Han JY, Xian Z, Zhang YS, Liu J, Liang AH. 2019. Systematic overview of aristolochic acids: nephrotoxicity, carcinogenicity, and underlying mechanisms. Front Pharmacol. 10(17):648.

Hassanen, Eman I, Khalaf A-AA, Zaki AR, Ibrahim MA, Galal MK, Farroh KY, Azouz RA. 2021. Ameliorative effect of ZnO-NPs against bioaggregation and systemic toxicity of lead oxide in some organs of albino rats. Environ Sci Pollut Res. doi:10.3389/fphys.2021.599114

Hu H, Tian M, Ding C, Yu S. 2019. The C/EBP homologous protein (CHOP) transcription factor functions in endoplasmic reticulum stress-induced apoptosis and microbial infection. Front Immunol. 9:3083.

Hu X, Chi Q, Liu Q, Wang D, Zhang Y, Li S. 2019. Atmospheric H2S triggers immune damage by activating the TLR-7/MyD88/NF-κB pathway and NLRP3 inflammasome in broiler thymus. Chemosphere. 237: 124427.

Huang Q, Li F, Liu X, Li W, Shi W, Liu F-F, O'Sullivan B, He Z, Peng Y, Tan A-C, et al. 2011. Caspase 3-mediated stimulation of tumor cell repopulation during cancer radiotherapy. Nat Med. 17(7):860–866.

Hyung S, Kim H. 2018. Inhibitory effect of astaxanthin on oxidative stress-induced mitochondrial dysfunction-a mini-review. Nutrients. 10: (9):1137.

Jiang X, Feng X, Huang H, Liu L, Qiao L, Zhang B, Yu W. 2017. The effects of rotenone-induced toxicity via the NF-κB-iNOS pathway in rat liver. Toxicol Mech Methods. 27(4):318–325.

Khalaf AA, Ibrahim MA, Galal MK, Abdallah AA, Mansour R, Afify MM. 2020. The protective effects ofTerminalia laxifloraextract on hepato-nephrotoxicity induced by fipronil in male rats. Environ Sci Pollut Res. 27(31):39507–39515.

Ku B, Liang C, Jung JU, Oh BH. 2011. Evidence that inhibition of BAX activation by BCL-2 involves its tight and preferential interaction with the BH3 domain of BAX. Cell Res. 21(4):627–641.

Lakhani SA, Masud A, Kuida K, Porter GA, Booth CJ, Mehal WZ, Inayat I, Flavell RA. 2006. Caspases 3 and 7: Key Mediators of Mitochondrial Events of Apoptosis. Science. 311(5762):847–851.

Lauber K, Bohn E, Kröber SM, Xiao Y-j, Blumenthal SG, Lindemann RK, Marini P, Wiedig C, Zobywalski A, Baksh S, et al. 2003. Apoptotic cells induce migration of phagocytes via caspase-3-mediated release of a lipid attraction signal. Cell. 113(6):717–730.

Li J, Chang X, Shang M, Niu S, Zhang W, Zhang B, Huang W, Wu T, Zhang T, Tang M, et al. 2021. Mitophagy-lysosomal pathway is involved in silver nanoparticle-induced apoptosis in A549 cells. Ecotoxicol Environ Saf. 208:111463.

Li YC, Tsai SH, Chen SM, Chang YM, Huang TC, Huang YP, Chang CT, Lee JA. 2012. Aristolochic acid-induced accumulation of methylglyoxal and Nε-(carboxymethyl)lysine: an important and novel pathway in the pathogenic mechanism for aristolochic acid nephropathy. Biochem Biophys Res Commun. 423(4):832–837.

Martinou JC, Youle R. 2011. Mitochondria in apoptosis: Bcl-2 family members and mitochondrial dynamics. Dev Cell. 21(1):92–101.

Mohamed RH, Tarek M, Hamam GG, Ezzat SF. 2019. Zoledronic acid prevents the hepatic changes associated with high fat diet in rats; the potential role of mevalonic acid pathway in nonalcoholic steatohepatitis. Eur J Pharmacol. 858:172469.

Ng AWT, Poon SL, Huang MN, Lim JQ, Boot A, Yu W, Suzuki Y, Thangaraju S, Ng CCY, Tan P, et al. 2017. Aristolochic acids and their derivatives are widely implicated in liver cancers in Taiwan and throughout Asia. Sci Transl Med. 9(412):eaan6446.

Oakes SA. 2020. Endoplasmic reticulum stress signaling in cancer cells. Am J Pathol. 190(5):934–946.

Ouyang L, Zhang Q, Ma G, Zhu L, Wang Y, Chen Z, Wang Y, Zhao L. 2019. New dual-spectroscopic strategy for the direct detection of aristolochic acids in blood and tissue. Anal Chem. 91(13):8154–8161.

Quan Y, Jin L, Luo K, Jin J, Lim SW, Shin YJ, Ko EJ, Chung BH, Yang CW. 2020. Assessment of nephrotoxicity of herbal medicine containing aristolochic acid in mice. Korean J Intern Med. 35(2):400–407.

Romanov V, Whyard TC, Waltzer WC, Grollman AP, Rosenquist T. 2015. Aristolochic acid-induced apoptosis and G2 cell cycle arrest depends on ROS generation and MAP kinases activation. Arch Toxicol. 89(1): 47–56.

Schwabe RF, Luedde T. 2018. Apoptosis and necroptosis in the liver: a matter of life and death. Nat Rev Gastroenterol Hepatol. 15(12): 738–752.

Singh R, Letai A, Sarosiek K. 2019. Regulation of apoptosis in health and disease: the balancing act of BCL-2 family proteins. Nat Rev Mol Cell Biol. 20(3):175–193.

Sinha K, Das J, Pal PB, Sil PC. 2013. Oxidative stress: the mitochondria-dependent and mitochondria-independent pathways of apoptosis. Arch Toxicol. 87(7):1157–1180.

Tanaka A. 2000. Chinese herb nephropathy in Japan presents adult-onset Fanconi syndrome: could different components of aristolochic acids cause a different type of Chinese herb nephropathy? Clin Nephrol. 53: 301–306.

Vanherweghem JL, Depierreux M, Tielemans C, Abramowicz D, Dratwa M, Jadoul M, Richard C, Vandervelde D, Verbeelen D, Vanhaelen-Fastre R. 1993. Rapidly progressive interstitial renal fibrosis in young women: association with slimming regimen including Chinese herbs. Lancet. 341(8842):387–391.

Wang X, Han C, Cui YQ, Li SY, Jin GZ, Shi WY, Bao YZ. 2021. Florfenicol causes excessive lipid peroxidation and apoptosis induced renal injury in broilers. Ecotoxicol Environ Saf. 207:111282.

Wu CC, Bratton SB. 2013. Regulation of the intrinsic apoptosis pathway by reactive oxygen species. Antioxid Redox Signaling. 19(6):546–558.